Available online at www.sciencedirect.com

SCIENCE DIRECT®

Journal of Marine Systems 53 (2005) 197–216

JOURNAL OF MARINE SYSTEMS

www.elsevier.com/locate/jmarsys

A high order linear model for the prediction of internal lee waves at the main sill of the Strait of Gibraltar

J.J. Alonso del Rosario*, E. Andonegui Odriozola

Department of Applied Physics, Physical Oceanography, University of Cádiz, Polígono del Rio San Pedro s/n, 11510, Puerto Real, Cádiz, Spain

Received 26 September 2003; accepted 12 May 2004
Available online 21 September 2004

Abstract

A linear theory for the physical fields in the water column under the action of large amplitude internal lee waves at the main sill of the Strait of Gibraltar is developed. The procedure is a combination of the perturbation and normal modes methods in order to study steady resonant conditions. The lowest order linear approach of the methodology resumes the Taylor–Goldstein equation, which can reconstruct the main features of the observed fields but the high order approach gives the finest structure and sometimes the largest contributions. The role of the non-linear terms is investigated up to the second order taking into account the non-linear interactions between modes, leading to an effective reconstruction of the whole water column for the velocity field.

Keywords: Internal lee waves; Non-linear theory; Strait of Gibraltar

1. Introduction

The surface signatures associated to the interaction of flows with topography are well-known oceanographic phenomena and can be observed almost in any coast and straits of the Earth. The surface slicks consist in slight modulations of the free surface. They use to be organized in rectangular plumes aligned with the internal wave crests (La Violette and Lacombe, 1988; New and Pingree, 1992). If more energetic waves act, a chaotic sea with breaking short waves is observed in surface. They are commonly named *hervideros* (boiling waters) by the Spanish fishermen in clear reference to the observed behavior of the surface water. They were firstly reported in the Strait of Gibraltar and its surroundings by the Spanish Navy in 1787 and after by Purdy (1840) and it is cited as *streamers*. This last denomination is commonly used in the scientific literature.

Most of the works on internal waves in the Strait of Gibraltar has focused on the generation, propagation and release of the internal bore with critical conditions over Camarinal sill during maximum Mediterranean

* Corresponding author.
E-mail address: josejuan.alonso@uca.es (J.J. Alonso del Rosario).

0924-7963/$ - see front matter © 2004 Elsevier B.V. All rights reserved.
doi:10.1016/j.jmarsys.2004.05.029

outflow (Frasseto, 1964; Ziegenbein, 1969; Cavanie, 1972; La Violette et al., 1986; Armi and Farmer, 1988; Richez, 1994; Watson and Robinson, 1990; Brandt et al., 1996; Farmer and Armi, 1999). The small amplitude westward travelling waves produce a surface signature hardly to detect because interface deepens into the Atlantic Ocean. All of them are generated during spring tides.

There is another kind of internal wave named *unsteady large amplitude lee waves* (ILW from hereafter). They were firstly reported by Lott and Teitelbaum (1993a,b) for the mountain waves in the atmosphere. The first explicit reference with a full numerical model is due to Nakamura et al. (2000) and Nakamura and Awaji (2001). The first observation of ILW in the Strait of Gibraltar was reported by Bruno et al. (2002) and the basis for their modeling can be found in Alonso et al. (2003). However, the ILW have been found before by Lacombe and Richez (1984), La Violette and Lacombe (1988) and Richez (1994), among many others, but they did not distinguish them from the classical internal bore. Some consequences of the ILW can be found in Echevarría et al. (2002) and other interesting details about the role of solitons in mixing using a simplistic model can be found in Lenner-Cody and Franks (1999). The linear theory of hydrodynamic stability has been the main tool to study ILW stability (Kundu, 1990; Gill, 1982; Bogucki et al., 1999; Bruno et al., 2002; Alonso et al., 2003). It leads to a quite good description of the main features of the phenomenon throughout Sturm–Liouville-type equations. However, the non-linear terms must be included in order to make a more realistic approach. This work deals with the problems of including the non-linear terms by an analytical approach based on the combination of perturbation and normal modes techniques, so all the resulting equations will be linearized, with the obtention of linear forced equations for each order depending of the previous orders solutions. It will be shown that the first order linear approach will have the largest contributions to the velocity field.

The work is organized as follows. In Section 2, a brief review of data, survey and a conceptual model for ILW is given. Section 3 is devoted to the description of the theoretical model. In Section 4, the numerical results are presented and discussed. Finally, the conclusions are drawn in Section 5.

2. The survey, data and the conceptual frame for ILW

The survey was carried out in November 1998 at the Camarinal Sill (Strait of Gibraltar) in a real-time assessment of currents for drilling operations (Fig. 1). The hydrodynamic conditions for drilling need very low currents and the operation was performed in neap tides. Hence all the results are biased to such a condition. A ship-mounted ADCP was working continuously and a multiparameter probe when needed. A very intense internal activity was recorded with a large amount of observed surface slicks. Data for the tidal current prediction has been taken from the Gibraltar Experiment 94/96 from a 150 kHz upward-looking ADCP moored at the top of Camarinal sill during 2 years (Fig. 1). The harmonic constants for the generation of the tidal current prediction can be found in Alonso et al. (2003). The records of the upward-looking ADCP present maximum values of horizontal velocities of 4 m/s when filtering and decimated the data to 1 data/h. Hence the internal activity is not taken into account. The internal waves were classified as internal lee waves (Alonso et al., 2003) and it was demonstrated that it happened during subcritical conditions over the sill (Bruno et al., 2002; Alonso et al., 2003). The ILW occurs when a hydrodynamic perturbation happens and finds suitable conditions of stratification for its upward propagation.

When the amplitude grows very energetic, surface slicks are observed at the surface. In Alonso et al. (2003), it was proved that the perturbation is produced by the interaction flow–topography. In the same paper, two new and important concepts were also introduced. The first one is the *topographic criterion of its existence* which says that the wavelength of the ILW must be contained in the topography; otherwise, the internal wave will be damped. The second one is the existence of a *critical velocity*: for background velocities lesser than a certain critical velocity (in the Strait of Gibraltar is about 0.5 m/s directed towards the Atlantic Ocean), there is no enough forcing to trigger the process.

The conceptual model has been described in Alonso et al. (2003); however, a brief outline is

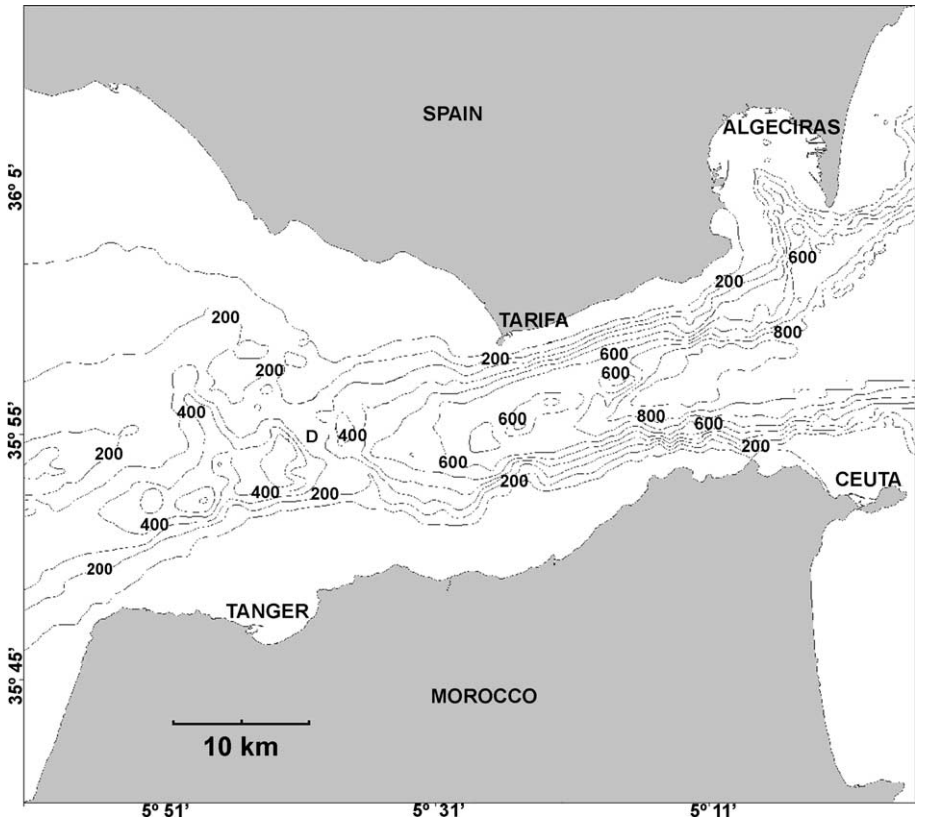

Fig. 1. The Strait of Gibraltar. The place where the ADCP was moored is marked with D. All the runs with the ship-mounted ADCP and CTD casts were performed around that point.

now given in order to fix some ideas. The generation of lee waves depends on the background velocity profile and on the stratification conditions (Hazel, 1972; Bruno et al., 2002; Alonso et al., 2003). The triggering mechanism is the interaction of the flow with the topography. The perturbation will propagate upward distorting all the physical fields. The composite Froude number is taken less than unity. Hence, the hydraulic jump has nothing to do with it. When an oscillatory (tidal) and unperturbed current flows over bottom topography in a stratified fluid, many kinds of hydrodynamic perturbation arise. Close to the bottom a perturbation occurs due to the advective terms in the equations of motion. If the conditions for its upward propagation are favorable ($\omega=Uk<N$, ω is the frequency of the internal wave, U the background velocity, k the wave number and N the root squared of the buoyancy frequency), a harmonic solution is obtained and it can propagate upward, otherwise the energy will be dissipated in the lower layer (damped solution) (Gill, 1982; Konyaev and Sabinin, 1992). With a zero relative velocity ($c=0$), the internal wave is arrested by the flow (Bogucki et al., 1999). When solving the numerical models, Nakamura et al. (2000) and Nakamura and Awaji (2001) did consider energy reflection at the surface; however, their results led to the conclusion that the energy reflection at the sea surface could be neglected. This is exact and introduces a difference with the previous and partially inaccurate conceptual model presented in Bruno et al. (2002) and Alonso et al. (2003). Then the conditions for resonance are observed and the internal wave will be amplified, producing a very strong mixing (see Echevarría et al., 2002) with a constant energy input radiating

from the bottom. The study of the vertical propagation angles can be found in Alonso et al. (2003) following the Garrett and Munk (1972) scheme. Because the tidal forcing is the driving force of the process and it is time-dependent, the ILW must be named *unsteady lee waves* (Nakamura et al., 2000) and they will occur as pulses (Alonso et al., 2003). Because the ILWs occur in subcritical conditions, the ILW and the internal bore in the Strait of Gibraltar are excluding and alternating processes.

Four cases were selected for this study (Table 1). They correspond to those moments reported in Alonso et al. (2003) in which the ILW activity was detected. A linear model gave the wavelengths detailed in Table 1. Only the wavelengths longer than 100 m have been included.

Table 1
Selected time moments for the computations of the velocity field

Case	Time (GMT)	Wavelength
a	11:15 26/11/1998	871,156
b	09:45 27/11/1998	959,168,115
c	01:00 29/11/1998	1270,119
d	15:30 29/11/1998	200,123,105

3. The theoretical model

The goal of this theoretical model is to study the velocity field produced by a hydrodynamic perturbation under resonant conditions. A perturbation technique is applied on a non-linear system of partial differential equations. The equations for the lowest order (linear) are isolated and reduced to the Taylor–Goldstein equation by means of normal modes. The resulting Sturm–Liouville problem is numerically solved. The solutions, the eigenfunctions or modes, are used to build a forcing function contained in the first order approach. The resulting system is reduced again by the same procedure to one single equation and it is numerically solved again. The process continues till reaching the required degree of approach. Although the formalism up to the second order is presented, it is enough to reach the first order in the computation in order to explain many of the features of the physical fields distorted by the action of the ILW.

3.1. Basic equations

The equations for a linear continuously stratified parallel flow with no rotation, zero viscosity, with Boussinesq condition and 2D with x-axis positive eastward and z-axis positive upward with the origin at a flat bottom are (Kundu, 1990):

$$\begin{aligned}
&\frac{\partial u}{\partial t}+u\frac{\partial u}{\partial x}+w\frac{\partial u}{\partial z}=-\frac{1}{\rho_0}\frac{\partial p}{\partial x}\\
&\frac{\partial w}{\partial t}+u\frac{\partial w}{\partial x}+w\frac{\partial w}{\partial z}=-\frac{1}{\rho_0}\frac{\partial p}{\partial z}-\frac{g}{\rho_0}\rho\\
&\frac{\partial \rho}{\partial t}+u\frac{\partial \rho}{\partial x}+w\frac{\partial \rho}{\partial z}=0\\
&\frac{\partial u}{\partial x}+\frac{\partial w}{\partial z}=0
\end{aligned} \tag{1}$$

where $u(x,z,t)$ and $w(x,z,t)$ are the horizontal and vertical velocities, respectively, $p(x,z,t)$ is the pressure field, $\rho(x,z,t)$ is the density field, g is the acceleration due to the gravity and ρ_0 is the density of reference. The flat bottom assumption is valid only when studying the near field. If the medium or the far field is to be studied, the theory must be drastically modified. Assuming that the horizontal velocity and density can be decomposed in a

horizontally constant background state and a perturbation due to the action of internal waves, the following set of equations will be considered:

$$\begin{aligned}
&\frac{\partial u}{\partial t}+u\frac{\partial u}{\partial x}+w\frac{\partial u}{\partial z}+U\frac{\partial u}{\partial x}+w\frac{dU}{dz}=-\frac{1}{\rho_0}\frac{\partial p}{\partial x}\\
&\frac{\partial w}{\partial t}+u\frac{\partial w}{\partial x}+w\frac{\partial w}{\partial z}+U\frac{\partial w}{\partial x}=-\frac{1}{\rho_0}\frac{\partial p}{\partial z}-\rho\frac{g}{\rho_0}.\\
&\frac{\partial \rho}{\partial t}+u\frac{\partial \rho}{\partial x}+w\frac{\partial \rho}{\partial z}+U\frac{\partial \rho}{\partial x}-wN^2\frac{\rho_0}{g}=0\\
&\frac{\partial u}{\partial x}+\frac{\partial w}{\partial z}=0
\end{aligned} \tag{2}$$

For the derivation of the successive approximations, all variables are expanded as:

$$\zeta=\zeta^{(0)}+\varepsilon\zeta^{(1)}+\varepsilon^2\zeta^{(2)}+\ldots \tag{3}$$

where $\zeta=\{u,w,p,\rho\}$. The expansion was performed till the second power of ε. The ε parameter is defined as the quotient between the amplitude of the incoming tide and the depth of the area under study and takes the value of 1/300=0.0333.

3.2. Lowest order solution (0-order)

The lowest order solution is achieve substituting Eq. (3) onto Eq. (2) and dropping all the terms multiplied by ε^i with $i>0$. The resulting system is well known and can be found in many references (i.e. Kundu, 1990; Gill, 1982):

$$\begin{aligned}
&\frac{\partial u^{(0)}}{\partial t}+U\frac{\partial u^{(0)}}{\partial x}+w^{(0)}\frac{dU}{dz}=-\frac{1}{\rho_{(0)}}\frac{\partial p^{(0)}}{\partial x}\\
&\frac{\partial w^{(0)}}{\partial t}+U\frac{\partial w^{(0)}}{\partial x}=-\frac{1}{\rho_0}\frac{\partial p^{(0)}}{\partial z}-\frac{g}{\rho_0}\rho^{(0)}\\
&\frac{\partial \rho^{(0)}}{\partial t}+U\frac{\partial \rho^{(0)}}{\partial x}-w^{(0)}N^2\frac{\rho_0}{g}=0\\
&\frac{\partial u^{(0)}}{\partial x}+\frac{\partial w^{(0)}}{\partial z}=0
\end{aligned} \tag{4}$$

where the superscript (0) stands for the lowest order approach. Taking normal modes, it is easy to get the Taylor–Goldstein equation that plays an important role in the study of hydrodynamic instabilities (Kundu, 1990; Konyaev and Sabinin, 1992):

$$\hat{\psi}^{(0)}_{zz}+q(z)\hat{\psi}^{(0)}=k^2\hat{\psi}^{(0)} \tag{5}$$

where subscripts stand for derivatives, $\hat{\psi}$ is the complex amplitude of the stream function, k is the wave number, and the potential function is

$$q(z)=\frac{N^2}{(U-c)^2}-\frac{U_{zz}}{(U-c)} \tag{6}$$

where c is the phase speed of the internal wave. Eq. (5), together with the boundary conditions $\hat{\psi}(0)=\hat{\psi}(h)=0$, is a classical fixed end-point Sturm–Liouville problem (Levitan, 1987) where the solutions are the eigenvectors, $\hat{\psi}_n$,

and their correspondent eigenvalues, k_n^2. For an arbitrary buoyancy frequency and background velocity profile (i.e. for an arbitrary $q(z)$ function), Eq. (5) must be solved numerically. If the interest is on internal waves that can be resonant, this is equivalent to say that the attention is focused on steady ILW, hence a zero relative phase velocity, c=0 (Bogucki et al., 1999; Nakamura et al., 2000; Nakamura and Awaji, 2001; Bruno et al., 2002; Alonso et al., 2003), is considered.

Once the numerical solution is obtained, the following expressions recover all the fields for the steady state perturbed velocity and density fields:

$$\begin{aligned} \rho_n^{(0)}(x,z) &= \hat{\rho}_n(z)\cos(kx) \\ u_n^{(0)}(x,z) &= \hat{u}_n(z)\cos(kx) \\ w_n^{(0)}(x,z) &= i\hat{w}_n(z)\sin(kx) \end{aligned} \tag{7}$$

where i is the imaginary number and the equations for the amplitudes of the velocity and density fields are:

$$\begin{aligned} \hat{\rho}_n(z) &= -C\frac{\rho_0 N^2}{gU}\hat{\psi}_n^{(0)}(z) \\ \hat{u}_n(z) &= -C\frac{\partial\hat{\psi}_n^{(0)}(z)}{\partial z} \\ \hat{w}_n(z) &= -iCk\hat{\psi}_n^{(0)}(z) \end{aligned} \tag{8}$$

where C is an arbitrary constant that must be fitted from observations and it can be selected equal to the observed amplitude of the isohalines, isotherms or isopicnals oscillations.

3.3. Next to lowest order solution

The first order linear solution is achieved by repeating the same procedure dropping all the terms multiplied by ε^2 and higher powers in the expansion. The first order linear system is:

$$\begin{aligned} &\frac{\partial u^{(1)}}{\partial t} + U\frac{\partial u^{(1)}}{\partial x} + w^{(1)}\frac{dU}{dz} = -\frac{1}{\rho_{(0)}}\frac{\partial p^{(1)}}{\partial x} + b_0^w \\ &\frac{\partial w^{(1)}}{\partial t} + U\frac{\partial w^{(1)}}{\partial x} = -\frac{1}{\rho_0}\frac{\partial p^{(1)}}{\partial z} - \frac{g}{\rho_0}\rho^{(1)} + b_0^w \\ &\frac{\partial \rho^{(1)}}{\partial t} + U\frac{\partial \rho^{(1)}}{\partial x} - w^{(1)}N^2\frac{\rho_0}{g} = +b_0^\rho \\ &\frac{\partial u^{(1)}}{\partial x} + \frac{\partial w^{(1)}}{\partial z} = 0 \end{aligned} \tag{9}$$

With

$$\begin{aligned} b_0^u(x,z) &= -\left(u^{(0)}\frac{\partial u^{(0)}}{\partial x} + w^{(0)}\frac{\partial u^{(0)}}{\partial z}\right) = -\underline{u}^{(0)}\nabla u^{(0)} \\ b_0^w(x,z) &= -\left(u^{(0)}\frac{\partial w^{(0)}}{\partial x} + w^{(0)}\frac{\partial w^{(0)}}{\partial z}\right) = -\underline{u}^{(0)}\nabla w^{(0)} \\ b_0^\rho(x,z) &= -\left(u^{(0)}\frac{\partial \rho^{(0)}}{\partial x} + w^{(0)}\frac{\partial \rho^{(0)}}{\partial z}\right) = -\underline{u}^{(0)}\nabla \rho^{(0)} \end{aligned} \tag{10}$$

where subscripts and superscripts (0) and (1) stand for the lowest order and first order linear solution, respectively. The underline terms denote vectors. Notice that Eq. (9) is the same as Eq. (4) with additional terms (Eq. (10))

except in the continuity. The non-linear interactions between the modes of the velocities and density are grouped in the terms of Eq. (10). Taking again normal modes and after a simple algebra, it is easy to get a single equation similar to Eq. (5):

$$\hat{\psi}_{zz}^{(1)} + q(z)\hat{\psi}^{(1)} = l^2\hat{\psi}^{(1)} + Q(z) \tag{11}$$

where l is the wave number, the definition of the potential function stands (Eq. (6)) and the forcing function is:

$$Q(z) = -\frac{g}{\rho_0 U(z)}\left(\psi_z^{(0)}\rho^{(0)} + \psi^{(0)}\rho_z^{(0)}\right) - \frac{1}{U(z)}\left(\psi_z^{(0)}\psi_{zz}^{(0)} - \psi^{(0)}\psi_{zzz}^{(0)}\right) \tag{12}$$

In the development of Eqs. (11) and (12), a zero relative phase velocity has been assumed. Eq. (11) together with the boundary conditions, $\hat{\psi}(z{=}0){=}\hat{\psi}(z{=}{-}h){=}0$, is a *forced Sturm–Liouville problem* that must be solved numerically. The forcing function, $Q(z)$, can be understood as the deflection from the equilibrium position of the stream lines (from an example of Courant and Hilbert, 1989a,b for the oscillations of a string) and takes into account the non-linear interaction between the modes of the stream function and density. Once the solution is achieved, the velocity field is computed in a similar way as that of the linear solution. The resulting amplitudes are computed combining Eqs. (3) and (8), multiplying the integration constant introduced in Section 3.2 and the small parameter ε used in the power expansion Eq. (3) and then considering Eq. (8).

3.4. Second order linear solution

The next step is building up the second order approach. The obtained linear system is

$$\begin{aligned}
&\frac{\partial u^{(2)}}{\partial t} + U\frac{\partial u^{(2)}}{\partial x} + w^{(2)}\frac{dU}{dz} = -\frac{1}{\rho_{(0)}}\frac{\partial p^{(2)}}{\partial x} + b_{01}^{u}\\
&\frac{\partial w^{(2)}}{\partial t} + U\frac{\partial w^{(2)}}{\partial x} = -\frac{1}{\rho_0}\frac{\partial p^{(2)}}{\partial z} - \frac{g}{\rho_0}\rho^{(2)} + b_{01}^{w}\\
&\frac{\partial \rho^{(2)}}{\partial t} + U\frac{\partial \rho^{(2)}}{\partial x} - w^{(2)}N^2\frac{\rho_0}{g} = b_{01}^{\rho}\\
&\frac{\partial u^{(2)}}{\partial x} + \frac{\partial w^{(2)}}{\partial z} = 0
\end{aligned} \tag{13}$$

With

$$\begin{aligned}
b_{01}^{u}(x,z) &= -\left(\varepsilon^{-1}\,\underline{u}^{(0)}\,\underline{\nabla}\,u^{(0)} + \underline{u}^{(0)}\,\underline{\nabla}\,u^{(1)} + \underline{u}^{(1)}\,\underline{\nabla}\,u^{(0)}\right)\\
b_{01}^{w}(x,z) &= -\left(\varepsilon^{-1}\,\underline{u}^{(0)}\,\underline{\nabla}\,w^{(0)} + \underline{u}^{(0)}\,\underline{\nabla}\,w^{(1)} + \underline{u}^{(1)}\,\underline{\nabla}\,w^{(0)}\right)\\
b_{01}^{\rho}(x,z) &= -\left(\varepsilon^{-1}\,\underline{u}^{(0)}\,\underline{\nabla}\,\rho^{(0)} + \underline{u}^{(0)}\,\underline{\nabla}\,\rho^{(1)} + \underline{u}^{(1)}\,\underline{\nabla}\,\rho^{(0)}\right)
\end{aligned} \tag{14}$$

where the meaning of all the symbols is understood. It must be noticed the great influence of the lowest order solution whose terms are multiplied by ε^{-1}, and recalling the expressions of the forcing (Eq. (10)) onto the new forcing terms (Eq. (14)): $b_0^u(x,z) = \underline{u}^{(0)}\,\underline{\nabla}\,u^{(0)}; b_0^w(x,z) = \underline{u}^{(0)}\,\underline{\nabla}\,w^{(0)}; b_0^\rho(x,z) = \underline{u}^{(0)}\,\underline{\nabla}\,\rho^{(0)}$. In addition, the non-linear interaction between the zero and first order linear solutions is contemplated in Eq. (14). By means of the same algebra as that of above, the following equation is reached for the second order:

$$\hat{\psi}_{zz}^{(2)} + q(z)\hat{\psi}^{(2)} = m^2\hat{\psi}^{(2)} + R(z) \tag{15}$$

where m is the wave number and the forcing function $R(x,z)$ is defined as:

$$R(z) = \frac{-1}{U(z)} \left(\begin{array}{l} \varepsilon^{-1}\hat{\psi}_z^{(0)}\hat{\psi}_{zz}^{(0)} - \varepsilon^{-1}\hat{\psi}^{(0)}\hat{\psi}_{zzz}^{(0)} + \hat{\psi}_{zz}^{(0)}\hat{\psi}_z^{(1)} + \hat{\psi}^{(0)}\hat{\psi}_{zzz}^{(1)} + \hat{\psi}_{zz}^{(1)}\hat{\psi}_z^{(0)} + \hat{\psi}^{(1)}\hat{\psi}_{zzz}^{(0)} + \\ \varepsilon^{-1}\hat{\psi}_z^{(0)}\rho^{(0)} - \varepsilon^{-1}\hat{\psi}^{(0)}\rho_z^{(0)} + \hat{\psi}_z^{(0)}\rho^{(1)} - \hat{\psi}^{(0)}\rho_z^{(1)} + \hat{\psi}_z^{(1)}\rho^{(0)} - \hat{\psi}^{(1)}\rho_z^{(0)} \end{array} \right) \tag{16}$$

taking into account again the non-linear interactions between modes of the lowest and first order solutions.

4. Numerical experiments, results and discussion

The best approach to solve this problem is developing a full non-linear tri-dimensional numerical model. This has been done partially by Nakamura et al. (2000) and Nakamura and Awaji (2001) with a bi-dimensional model. In the present study, we have adopted a more simplified approach with the objective of predicting the velocity field accurately, not exactly, but very fast. With this, the evolution problem is divided in many steady problems although sometimes could be unrealistic. Hence the background velocity and density fields are steady in each profile. The results will be the steady velocity field for each considered case.

4.1. Background velocity and buoyancy profiles

The study is focused in the period November 20th–30th, 1998 when a survey was performed (Alonso et al., 2003). Because the ILW occurs during neap tides condition and Mediterranean outflow, all the results are biased to such a condition (Bruno et al., 2002; Alonso et al., 2003). Some plots of the velocity field can be found in the two mentioned references and the considered moments for the computation (detailed in Table 1) have been selected from the paper of Alonso et al. (2003) when the internal waves were observed. The four vertical profiles of background velocities are presented in Fig. 2a. They have been obtained from the harmonic prediction of the currents following Foreman (1998).

The buoyancy profile is computed from the density profile (Bruno et al., 2002; Alonso et al., 2003). Since the survey was carried out during neap tides, the density and buoyancy profiles are representative of only such a tidal state. The density profile, without the action of internal waves, responds to a more or less constant vertical structure that can be described in terms of:

$$\rho(z) = \rho_0 + \frac{\rho_a}{\left(1 + \exp\left(-\frac{(z-\rho_{z_0})}{\rho_b}\right)\right)^{\rho_c}}$$

From observed CTD profiles, the mean computed parameters are ρ_a=3.36, ρ_b=−10.08, ρ_c=1.29 and ρ_0=1026.5 (Fig. 2b). The depth of the interface was taken from the vertical profile of background velocity.

Because one of the main problems at the Strait of Gibraltar is the location of the depth of the interface, it is necessary to say some words about it. The most common depth for the interface is where the 37.5 PSU isohaline is located, but because the CTD during the survey was not working continuously some approach to it is needed. In Bruno et al. (2002) and Alonso et al. (2003), the depth of the maximum shear was used successfully as an estimator of the depth of the interface. This is in agreement with Tsimplis and Bryden (2000) who found a difference of 8 m between the interface and the maximum shear depths.

4.2. Linear solution

After building the potential function (Eq. (6)), the linear solution is found by solving the Sturm–Liouville problem (Eq. (5)). This can be done by several numerical standard methods. Among them is that described in Henrici (1962) and the SLEIGN program (Bailey et al., 1991). The first one has problems with the round off errors and the second minimizes them for the smallest eigenvalue. Although formally the linear problem has infinite solutions, some wavelengths are only physically reliable. The *topographic criterion of its existence* was applied (Alonso et al., 2003). With this, the linear solution has the wave-

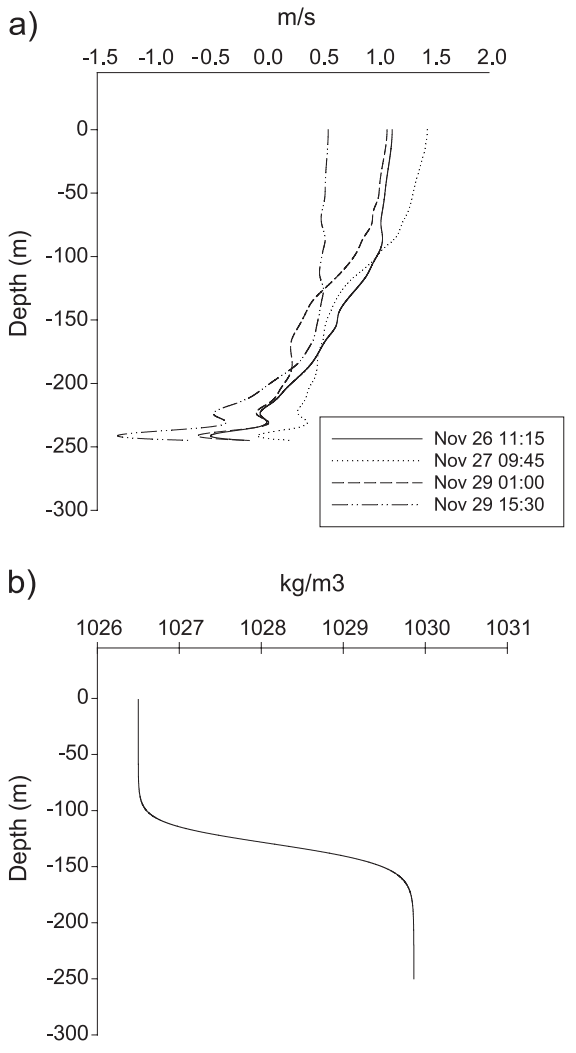

Fig. 2. (a) Vertical profiles of background velocities (m/s) for the four selected moments of Table 1. (b) Vertical profile of density (look the same for the selected moments with variations in the depth of the interface).

lengths detailed in Table 1. Eigenfunctions shorter than 100 m have not been considered.

Some words about the checking of the numerical solution are needed. The vertical profiles of the background velocity present zero crosses. Even if a different value of celerity, c, was considered, the term $U(z)-c$ would be zero somewhere in depth. In those points, the potential $q(z)$ (Eq. (6)) becomes infinity and $\psi_{zz}^{(0)}$ presents a discontinuity. In classical mechanics, this problem has no easy solution. The only approach consists in considering two opposite travelling wave packets (Messiah, 1962). This highly theoretical line is left for further works. However, the problem has been solved in Quantum Mechanics. This corresponds to the case of infinitely deep potential wall and the check point is that the solution of the Sturm–Liouville problem must be zero where the potential tends to infinity (Messiah, 1962). This is known as the tunnel effect. This has been verified in the process of the numerical solving. In the context of this study, this is read as the interface is a non-permeable barrier for the interchange of momentum across it. This is in agreement with the formulation of the theoretical model since the viscosity has not been taken into account.

Considering Eqs. (7) and (8) and selecting the integration constant as the maximum possible amplitude that the ILW can reach in the Strait of Gibraltar (about C=100 m), the linear reconstructed fields are shown in Fig. 3a–d for the horizontal velocity. The intensity is greater than 2 m/s for all cases without taking into account the background velocity. The vertical velocity is presented in Fig. 4a–d and the intensity is about 1 m/s. In order to check these values, the statistics of the current meters moored in the Gibraltar Experiment 84/86 (Pillsbury et al., 1987) prescribe maximum values for the horizontal velocity about 2 m/s for the two moorings placed several kilometres to the north and south of the Camarinal sill. It must be noticed that the values have been averaged by the instruments and smoothen by numerical filtering, so the internal activity was not taken into account. The velocity field presented in Figs. 3 and 4 and the linear superposition of all the modes detailed in Table 1 have been considered. The effect of adding the higher oscillation modes is the loosing of the symmetry. Although the initial model is valid for small perturbations and the constant of integration seems quite large, Groeb (1948) gave two mathematical theorems showing the validity of Eq. (5) for long waves and large amplitudes. Hence, regardless of the value of the constant, it can be selected as large as needed. Notice the typical structure of the fields when an internal wave is acting and the high values of the vertical velocity field.

The streamers observed at the sea surface appear where a strong horizontal gradient of horizontal velocities as it was observed in Bruno et al. (2002). This can be easily located in Fig. 3a–d. Cases b and d

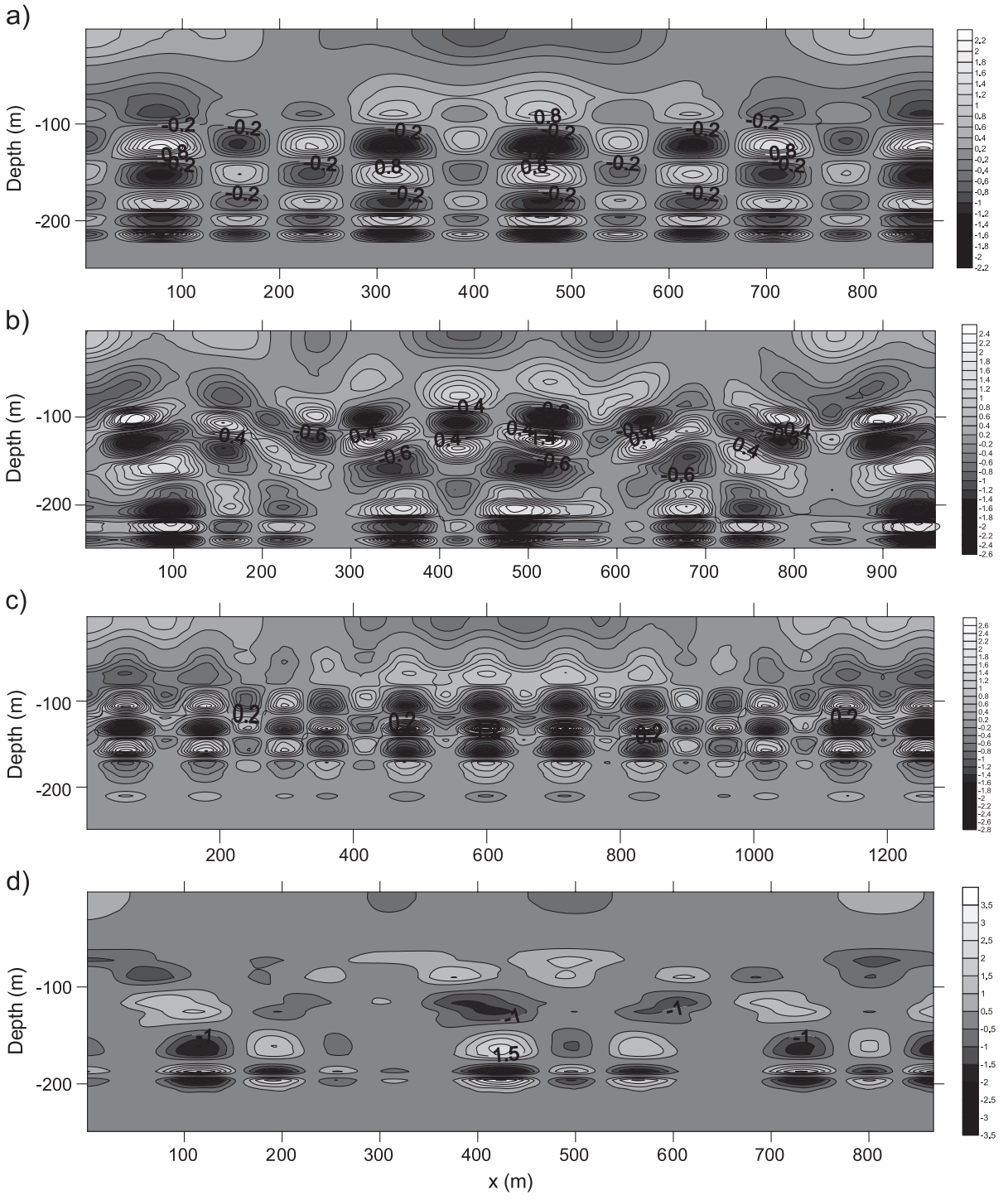

Fig. 3. Horizontal velocity field for the linear problem. The order of the figures follows that of Table 1.

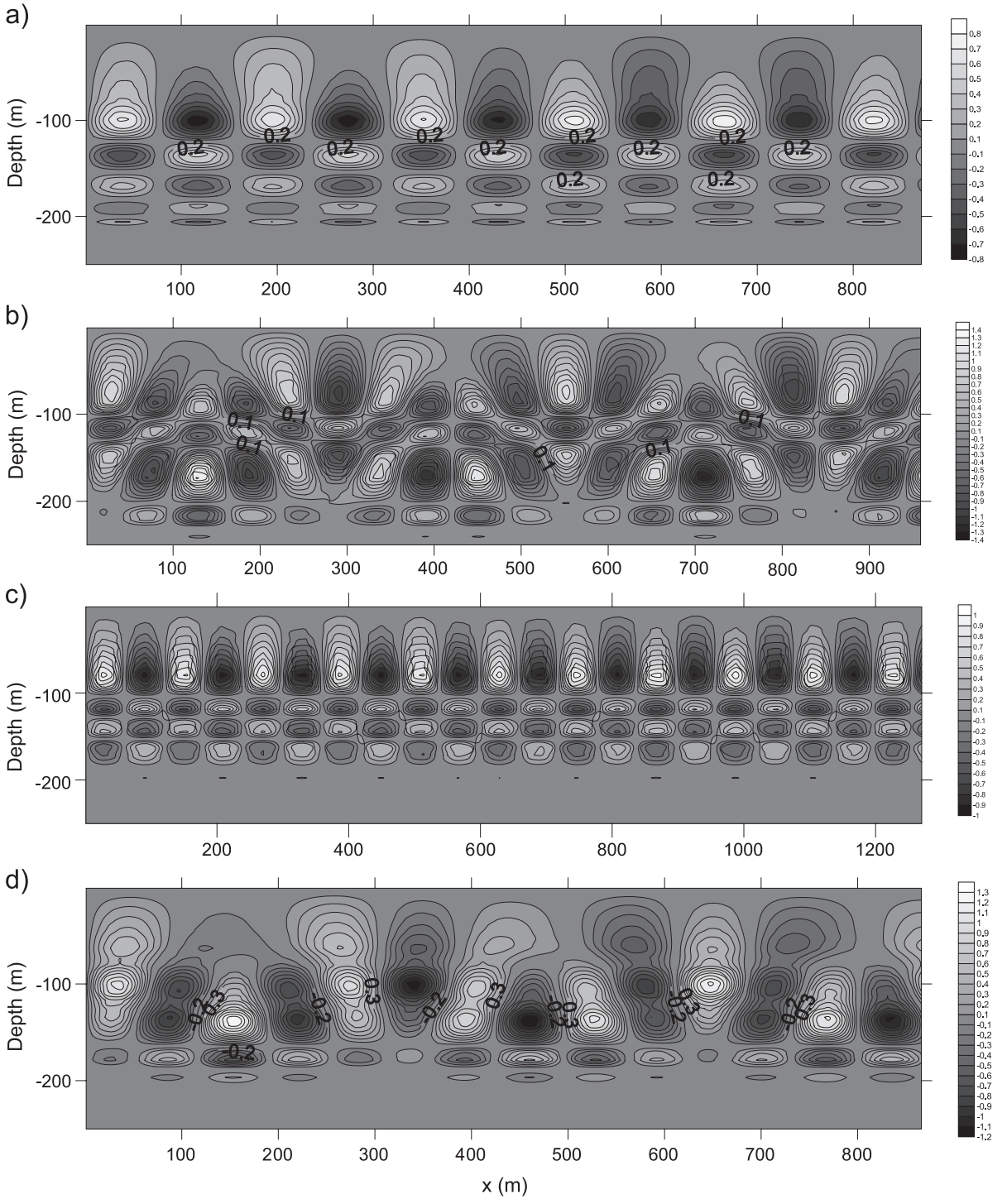

Fig. 4. Vertical velocity field for the linear problem. The order of the figures follows that of Table 1.

show a very intense internal activity with streamers irregularly spaced. Hence, the determination of the wavelength from the surface signature or from data taken at any depth, together with the small amount of data usually available, is not a trivial problem and it must be done carefully. A consequence of this is that the use of classical spectral analysis on XBT or velocity data could lead to biased results and modern techniques, as Maximum Entropy Spectral Analysis (Konyaev, 1990) has to be used. In case no surface manifestation be observed, the spectral analysis of surface signatures is not possible and must be done from ship-mounted ADCP data after a careful selection of the depth (see case d). In addition, different and contradictory results can be reached depending on the data for a selected depth to be spectrally analyzed. These reconstructions are in agreement with Bruno et al. (2002) and Alonso et al. (2003).

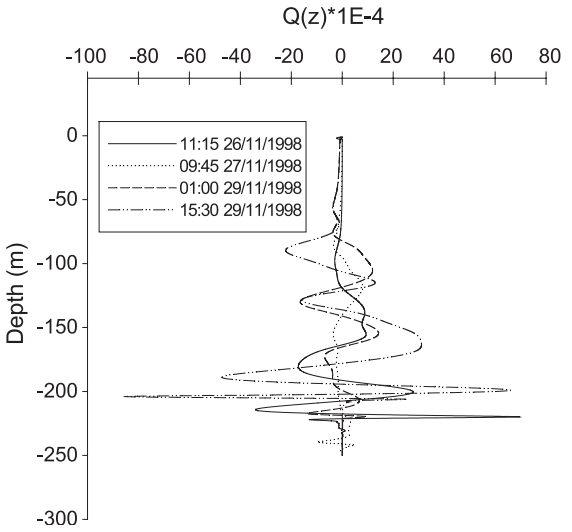

Fig. 5. Vertical structure of the forcing term for the selected cases of Table 1.

4.3. First order linear solution

The first order linear solution can be strictly reached by solving the Sturm–Liouville problem of Eq. (11). This can be done in terms of a Green's function (Courant and Hilbert, 1989a,b) with a very complicate numerical scheme. However, for this case it is not necessary because the first order linear contribution is computed for a given wavelength determined in the solution of the linear case. Hence a second order ordinary differential equation must be solved for the amplitude of the stream function. The resulting wavelength of the linear problem and the linear solution are used for the construction of the forcing function, $Q(z)$ (Eq. (12)). The stability of the solution is guaranteed by the verification of several theorems on stability detailed in Hayashi (1985). The vertical structure of the forcing function for the selected cases (Table 1) is presented in Fig. 5.

Integration of Eq. (11) for all cases was carried out by the Runge–Kutta–Felbergh method and the solution was to the selected depth levels following the algorithms found in Press et al. (1986). Fig. 6a and b presents the contribution to the horizontal velocity field of the first order linear solution for the two wavelengths detailed in Table 1. In Fig. 6, c and d are the same for the vertical velocity field. Fig. 7a presents the synthetic horizontal velocity field of the three acting modes for case b. Fig. 7b is the same for the vertical velocity. Fig. 8a and b has the same reading as that of Fig. 6, but for case c and Fig. 9 is the same as that of Fig. 7 but for case d. For the correct reading of the figures, the values must be multiplied for the power expansion parameter ε in order to obtain velocities expressed in m/s. It is not possible to predict a priori the structure of the first order linear solution for the horizontal and vertical velocity fields. Hence they must be computed and the researcher can find very small contributions (as it happens in the vertical velocity solution). Depending on the non-linear interaction between the modes which were taken into account in the forcing function, the first order linear solution will be concentrated at the bottom, at mid-water column or will spread in the whole water column.

From the numerical computations, the influence of the first order linear solution, having considered the non-linear interaction between modes, is very important and it is the main contribution to the horizontal velocity field induced by the ILWs. We have found that this contribution can have maximum values up to 0.5 m/s (about 25% for a single mode).

In practice, the high order contributions to the vertical velocity must be taken till the first linear contribution for each mode computed in the lowest order approach. Depending on the amplitude, up to

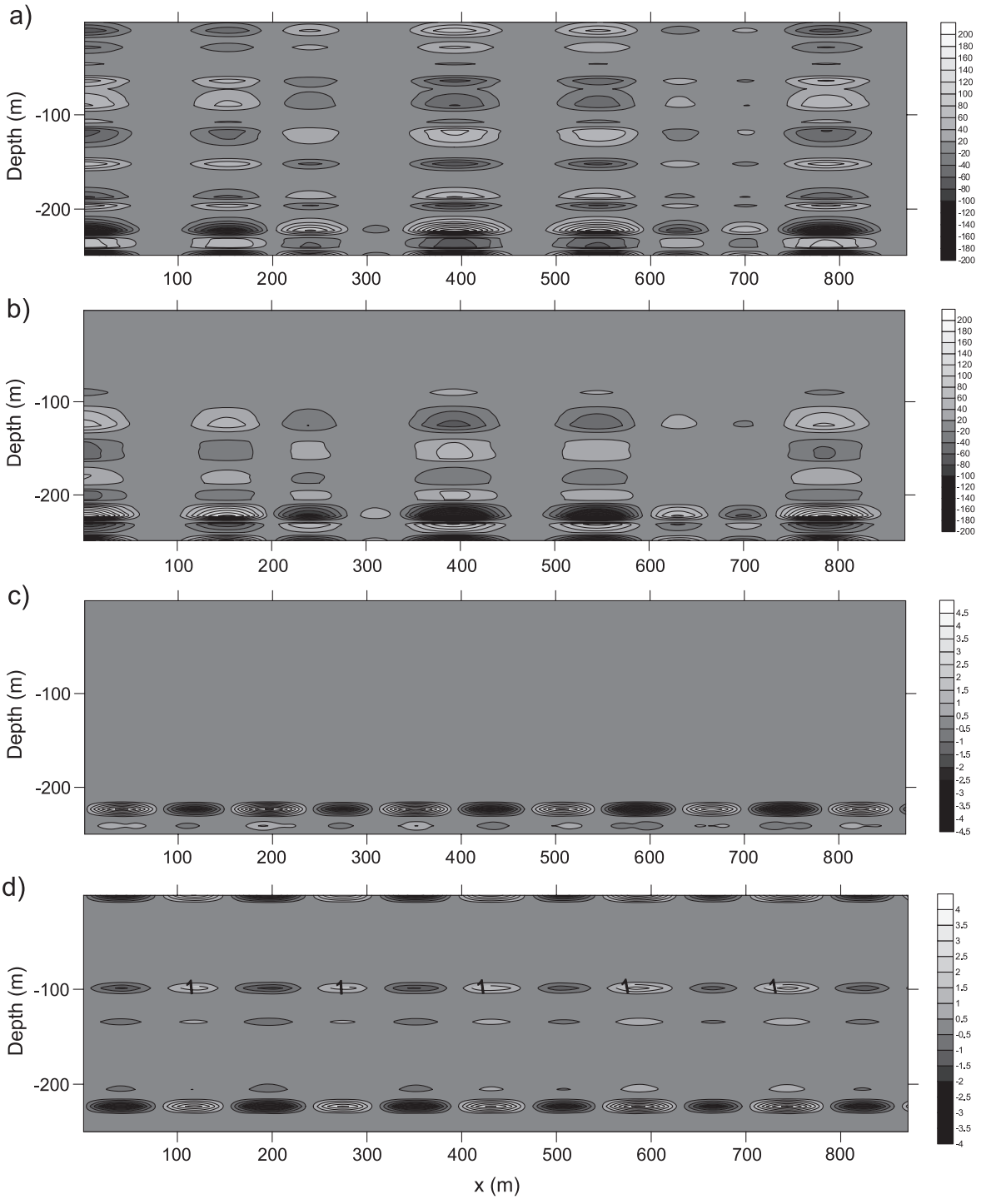

Fig. 6. First order linear solution. Figure a represents the first order linear solution for the horizontal velocity first mode of case a (Table 1). Figure b is the same for the second mode. Figures c and d are the same for the vertical velocity. The values must be multiplied by ε to be expressed in m/s.

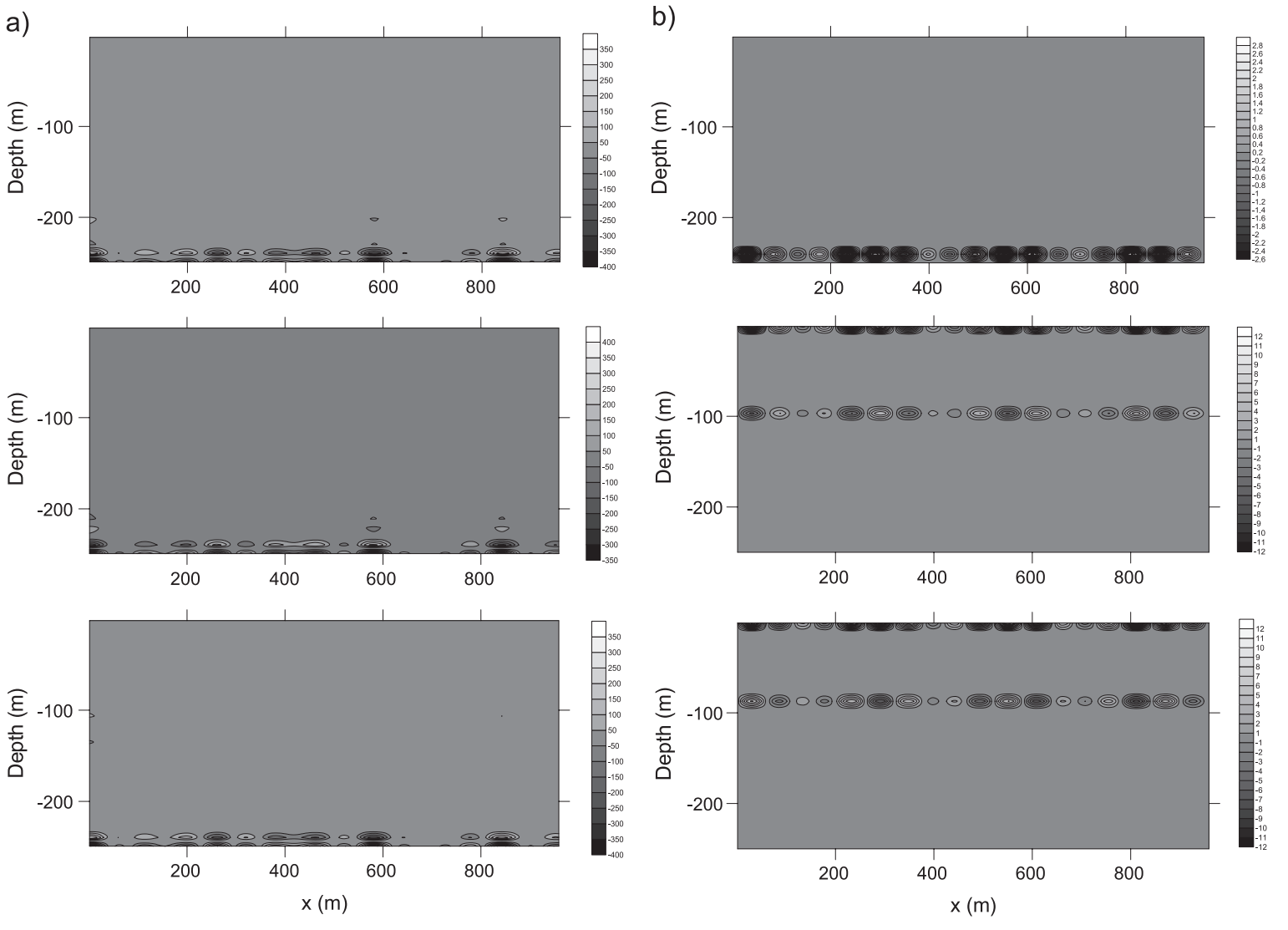

Fig. 7. Same legend as Fig. 6 for case b. Now three modes are available. Figure a is for the horizontal velocity and figure b for the vertical velocity. The values must be multiplied by ε to be expressed in m/s.

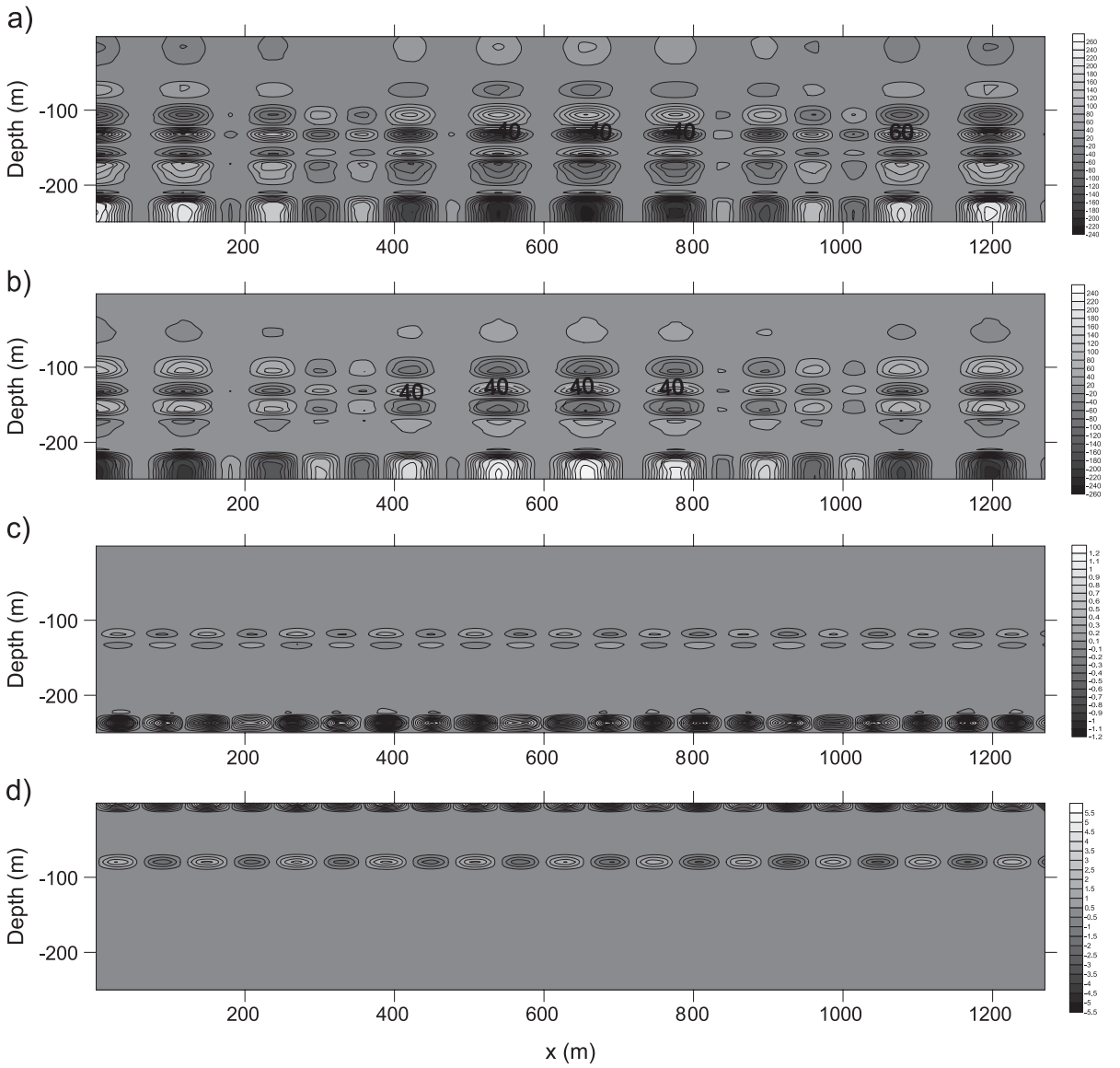

Fig. 8. Same legend as Fig. 6 for case c. The values must be multiplied by ε to be expressed in m/s.

the third mode can be necessary for the horizontal velocity field.

4.4. Second order linear solution

Although the formalism for the second order contribution has been presented, computed and analyzed for all cases, they have no influence on the final solution (less than 2%). So for practical purposes, the computation of the lowest and first order linear solutions is enough.

4.5. Final velocity field

The final velocity field is obtained from Eq. (3). For the horizontal velocity field, it is necessary to add the background velocity profile, and for the vertical velocity field, Eq. (3) stands.

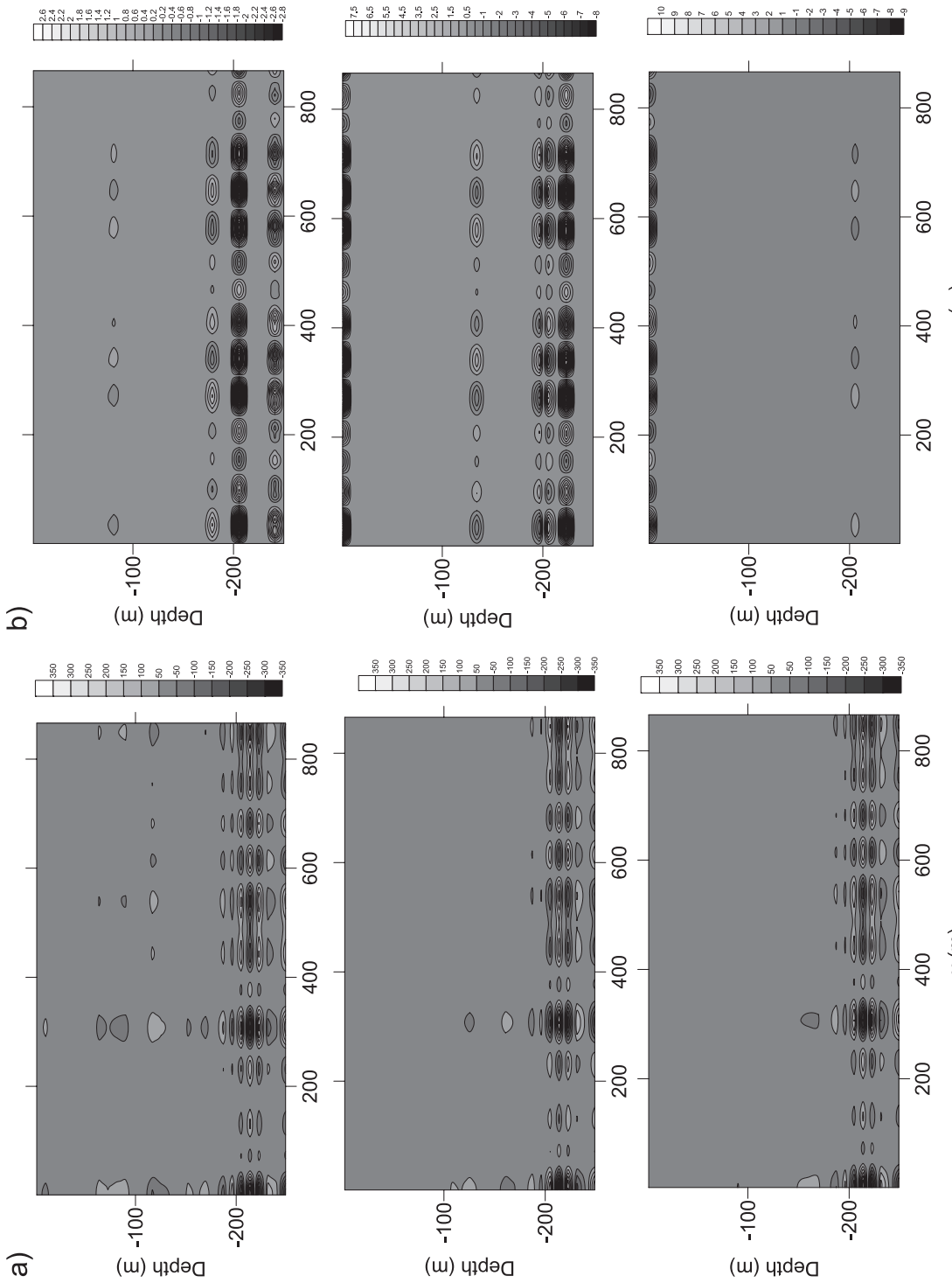

Fig. 9. Same legend as Fig. 7 for case d. The values must be multiplied by ε to be expressed in m/s.

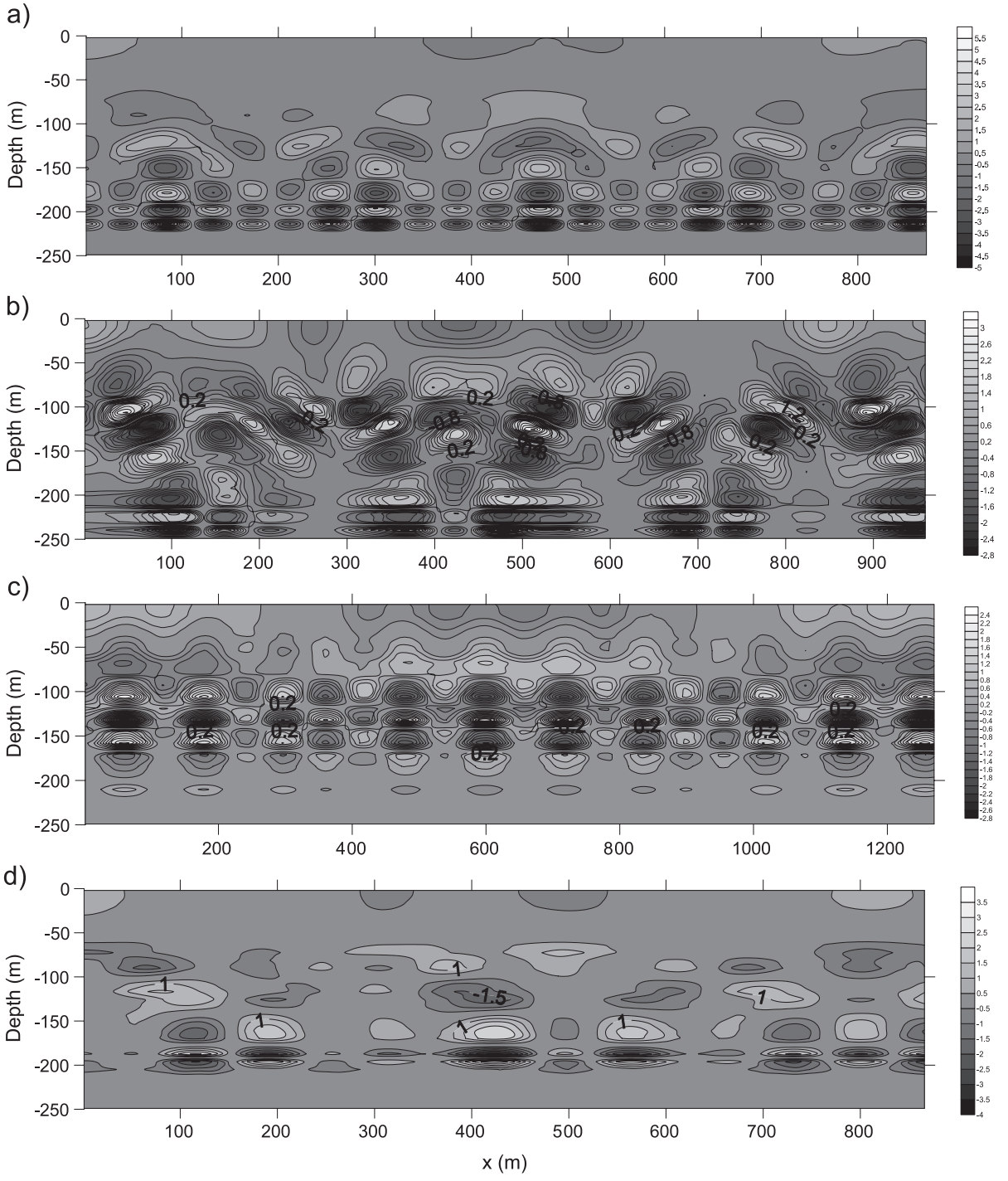

Fig. 10. Final horizontal velocity fields. Figures are presented in the same order as that of Table 1. Units are m/s.

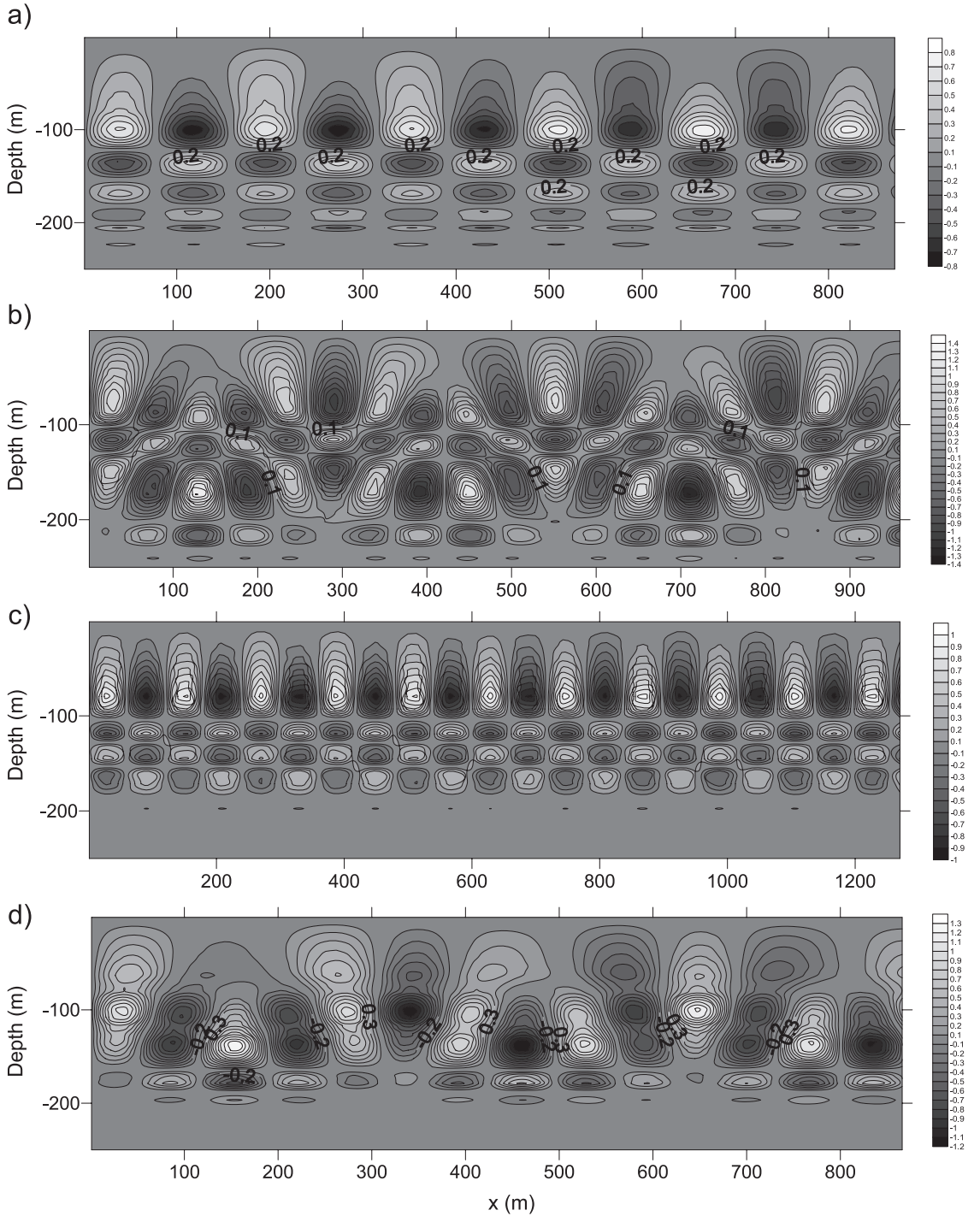

Fig. 11. Final vertical velocity fields. Figures are presented in the same order as that of Table 1. Units are m/s.

The resulting horizontal velocity fields for the four cases are presented in Fig. 10a–d and for the vertical velocity fields in Fig. 11a–d. The high order linear part contributes about 25% for each single mode. The effect of adding them is translated in an intensification of the currents. Recalling Section 2, the maximum values of the background current are about 4 m/s; when adding the contribution of each mode of the lowest order solution, the values of the horizontal velocity raise to more than 5 m/s. For more energetic processes, it is possible to obtain velocities higher than 8 m/s. For the vertical component, the velocities are up to 1 m/s for vertical velocities, and more chaotic internal velocity field can be observed. These are in very good agreement with the conclusions of Echevarría et al. (2002) and with the observed fields presented in Bruno et al. (2002) and Alonso et al. (2003).

We hope that further measurements when the internal events act confirm these theoretical results.

5. Conclusions

A linear second order formulation for the explanation of the spatial structure of the physical fields due to ILW in a water column is developed and applied to the main sill of the Strait of Gibraltar. By an analytical method based on perturbation and normal mode procedures, the Taylor–Goldstein equation is obtained as the lowest order, the highest orders are second order linear ordinary differential equations. All the problems are numerically solved. After the computation of the lowest order solution, the eigenfunctions are used to compute the forcing function needed to solve high order approach. The forcing terms take into account the non-linear interaction between modes. The first order linear approach represents up to the 25% of the lowest order solution for a single mode. When all the first order contributions are taken into account, high values of the horizontal velocity field are obtained, reaching maxima of about 10 m/s.

Although the second order linear solution is computed for all cases, they contribute about 2% and they can be neglected. With this, a first order model is enough for a very good description of the near field velocity close to the main sill of the Strait of Gibraltar.

Although the presented model is quite powerful and zero viscosity has been considered, there are two main directions for further works. The first is the inclusion of the viscosity in the model in order to investigate its effect, and the second is the use of a full non-linear numerical model for the main sill of the Strait of Gibraltar in order to explain the finest details of the velocity field and to scope in the fine structure of the phenomenon.

Acknowledgements

The authors are grateful to Dr. Concepción García from the Department of Applied Mathematics of the University of Cádiz for some interesting notes about stability and Γ-convergence. We are also grateful to the three anonymous referees; their accurate comments have really improved the original version of the manuscript.

References

Alonso, J.J., Bruno, M., Vázquez, A., 2003. On the influence of tidal hydrodynamic conditions in the generation of internal resonant waves at the main sill of the Strait of Gibraltar. Deep-Sea Res., Part 1 50, 1005–1021.

Armi, L., Farmer, D.M., 1988. The Flow of Mediterranean water through the Strait of Gibraltar. Prog. Oceanogr. 21, 1–105.

Bailey, P.B., Garbow, B.S., Kaper, H.G., Zetti, A., 1991. Trans. Math. Softw. 17 (4, December), 500–501.

Bogucki, D., Redekopp, L.G., Dickey, T., 1999. Sediment resuspension and mixing by resonantly generated internal solitary waves. J. Phys. Oceanogr. 27, 1181–1196.

Brandt, P., Alpers, W., Backhaus, J.O., 1996. Study of the generation and propagation of the internal waves in the Strait of Gibraltar using a numerical model and synthetic aperture radar images of the European ERS—a satellite. J. Geophys. Res. 101, 14252–14327.

Bruno, M., Alonso, J., Cózar, A., Vidal, J., Echevarría, F., Ruiz, J., Ruiz, A., 2002. The boiling water phenomena at Camarinal Sill, the Strait of Gibraltar. Deep-Sea Res., Part 2 49, 4097–4113.

Cavanie, A.G., 1972. Observations de fronts internes dans le detroit de Gibraltar pendant la Campagne Océanographique OTAN 1970 et interpretation des résultats par un modéle mathématique. Mém. Soc. Sci. Liége 6, 27–41.

Courant, R., Hilbert, D., 1989a. Methods in Mathematical Physics, vol. I. John Wiley and Sons, New York.

Courant, R., Hilbert, D., 1989b. Methods in Mathematical Physics, vol. II. John Wiley and Sons, New York.

Echevarría, F., Gómez, F., García Lafuente, J., Gorsky, G., Goutx, M., González, N., Bruno, M., García, C., Vargas, J.M., Picheral,

H., Striby, L., Alonso del Rosario, J., Reul, A., Cózar, A., Prieto, L., Jiménez-Gómez, F., Varela, M., 2002. Physical–biological coupling in the Strait of Gibraltar. Deep-Sea Res., Part 2 49, 4115–4130.

Farmer, D., Armi, L., 1999. The generation and trapping of solitary waves over topography. Science 283, 188–190.

Foreman, M.G.G., 1998. Manual for Tidal Heights and Prediction. Inst. of Ocean Sciences, Patricia Bay, Sidney, BC.

Frasseto, R., 1964. Short period vertical displacements of the upper layers in the Strait of Gibraltar. Tech. Rep. 30. SACLANT ASW, Res. Center, La Spezia, Italy.

Garrett, C.J.R., Munk, W.H., 1972. Space–time scales of internal waves. Geophys. Fluid Dyn. 3, 225–264.

Gill, A.E., 1982. Atmosphereocean dynamics. In: Donn, William L. (Ed.), International Geophysics Series. Academic Press, New York.

Groeb, P., 1948. Two fundamental theorems on gravity waves in inhomogeneous incompressible fluids. Physica XIV (5), 294–300.

Hayashi, C., 1985. Nonlinear Oscillations in Physical Systems. Princeton University Press, Princeton, NJ, pp. 392.

Hazel, P., 1972. Numerical studies of the stability of inviscid stratified shear flow. J. Fluid Mech. 5 (1), 39–62.

Henrici, P., 1962. Discrete variable methods in ordinary differential equations. John Wiley & Sons, New York.

Konyaev, K.V., 1990. Spectral Analysis of Physical Oceanographic Data. A.A. Balkema, Rotterdam. 200 pp.

Konyaev, K.V., Sabinin, K.D., 1992. Waves Inside the Ocean. Gidrometeoizdat. in Russian.

Kundu, P.J., 1990. Fluids Mechanics. Academic Press, New York.

Lacombe, H., Richez, C., 1984, Hydrography and currents in the Strait of Gibraltar. Office of Naval Research, Sea Straits Report 3, NORDA.

La Violette, P.E., Lacombe, H., 1988. Tidal induced pulses in the flow through the Strait of Gibraltar. Oceanol. Acta, SP, 13–17.

La Violette, P.E., Kinder, T.H., Green, D.W., 1986. Measurement of internal wave in the Strait of Gibraltar using shore based radar, Technical report 118. Naval Ocean Research and Development Activity, National Space Technology Laboratory, Bay of St. Louis, MO. 13 pp.

Lenner-Cody, C.E., Franks, P.J.S., 1999. Plankton patchiness in high-frequency internal waves. Mar. Ecol., Prog. Ser. 186, 59–66.

Levitan, B.M., 1987. Inverse Sturm–Liouville Problems. Colleage Press, Beijing, p. 240.

Lott, F., Teitelbaum, H., 1993. Topographic waves generated by a transient wind. J. Atmos. Sci. 50, 2607–2624.

Lott, F., Teitelbaum, H., 1993. Linear unsteady mountain waves. Tellus 45A, 201–220.

Messiah, A., 1962. Mecánica Cuántica, vol. I and vol. II. Ed Tecnos, Madrid, pp. 1078.

Nakamura, T., Awaji, T., 2001. A growth mechanism for topographic internal waves generated by an oscillatory flow. J. Phys. Oceanogr. 31, 2511–2524.

Nakamura, T., Awaji, T., Hatayama, T., Akitomo, K., Takizawa, T., Kono, T., Kawasaki, Y., Fukasawa, M., 2000. The generation of large-amplitude unsteady LEE waves by subinertial K1 tidal flow: a possible vertical mixing mechanism in the Kuril Strait. J. Phys. Oceanogr. 30, 1601–1621.

New, A., Pingree, R.D., 1992. Local generation of internal soliton packets in the central Bay of Biscay. Deep-Sea Res. 39, 1521–1534.

Pillsbury, R.D., Barstow, D., Bottero, J.S., Milleiro, C., Moore, B., Pittock, G., Root, D.C., Simpkins III, J., Still, R.E., Bryden, H., 1987. Gibraltar Experiment: Current measurements in the Strait of Gibraltar. Office of Naval Research, pp. 284. NR083-102.

Press, W.H., Flannery, B.P., Teukolsky, S.A., Vetterling, W.T., 1986. Numerical Recipes. Cambridge University Press, Cambridge.

Purdy, J., 1840. The New Sailing Directory for the Strait of Gibraltar and The Western Division of the Mediterranean Sea. HMSO.

Richez, C., 1994. Airborne synthetic aperture radar tracking of internal waves in the Strait of Gibraltar. Prog. Oceanogr. 33, 93–159.

Tsimplis, M., Bryden, H., 2000. Estimation of the transports through the Strait of Gibraltar. Deep-Sea Res., Part 1 47, 2219–2242.

Watson, G., Robinson, L.S., 1990. A study on internal wave propagation in the Strait of Gibraltar using shore-based radar images. J. Phys. Oceanogr. 20, 374–395.

Ziegenbein, J., 1969. Short internal waves in the Strait of Gibraltar. Deep-Sea Res. 16, 479–487.